

# Title goes here

D. Piras,<sup>1</sup>★ B. Joachimi,<sup>2</sup>

<sup>1</sup>*Dipartimento di Fisica “G. Galilei”, Università di Padova, via Marzolo 8, I-35131 Padova, Italy*

<sup>2</sup>*Department of Physics and Astronomy, University College London, Gower Street, London WC1E 6BT, UK*

4 April 2017

## ABSTRACT

This is a simple template for authors to write new MNRAS papers. The abstract should briefly describe the aims, methods, and main results of the paper. It should be a single paragraph not more than 250 words (200 words for Letters). No references should appear in the abstract.

**Key words:** keyword1 – keyword2 – keyword3

## 1 INTRODUCTION

### 1.1

This is a simple template for authors to write new MNRAS papers. See `mnras_sample.tex` for a more complex example, and `mnras_guide.tex` for a full user guide.

All papers should start with an Introduction section, which sets the work in context, cites relevant earlier studies in the field by ?, and describes the problem the authors aim to solve (e.g. ?).

## 2 DATA

In this work we have considered haloes from two different catalogues:

**The Millennium Simulation:** here we present a simulation of the growth of dark matter structure using 2,1603 particles, following them from redshift  $z = 127$  to the present in a cube-shaped region 2.230 billion light years on a side

**The Millennium-XXL Simulation (MXXL):** with a box side of 3 Gpc  $h^1$ , it was especially tailored to study massive haloes which can be only found in very large volumes. It

### 2.1 Figures and tables

Figures and tables should be placed at logical positions in the text. Don’t worry about the exact layout, which will be handled by the publishers.

Figures are referred to as e.g. Fig. 1, and tables as e.g. Table ??.

## 3 METHODOLOGY

To measure the correlation between the shapes of galaxy clusters and the density field we proceed as in van Uitert & Joachimi (2017),

★ E-mail: davide.piras@studenti.unipd.it

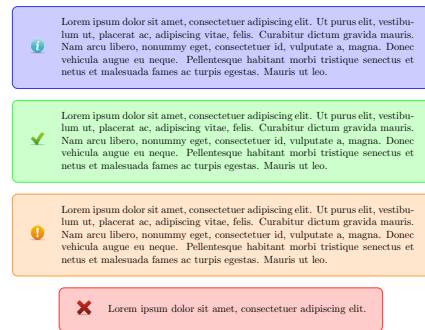


**Figure 1.** This is an example figure. Captions appear below each figure. Give enough detail for the reader to understand what they’re looking at, but leave detailed discussion to the main body of the text.

namely we define an estimator as a function of the comoving transverse distance  $R_p$  and the line-of-sight distance  $\Pi$ :

$$\hat{\xi}_{g+}(R_p, \Pi) = \frac{S_+ D_d}{D_s D_d} - \frac{S_+ R}{D_s R}, \quad (1)$$

where  $S_d D_d$  represents the correlation between cluster shapes and the density sample,  $D_s D_d$  the number of cluster shape - density pairs,  $S_d R$  the correlation between cluster shapes and random points and  $D_s R$  the number of cluster shape - random point pairs. We then integrate along the line of sight to obtain the total projected intrinsic alignment signal:

$$\hat{w}_{g+}(R_p) = \int_0^{\Pi_{max}} d\Pi \hat{\xi}_{g+}(R_p, \Pi); \quad (2)$$

throughout this work, we adopt  $\Pi_{max} = 60$  Mpc/h, a value large enough not to miss part of the signal but small enough not to pick up too much noise. \*\*\*ASK IF  $\Pi_{min} = 0$  IS CORRECT\*\*\*

We describe the intrinsic alignment signal by simplifying the model in [van Uitert & Joachimi \(2017\)](#), namely we assume:

$$w_{g+}(R_p, M) = A_{IA}(M) b_g(M) w_{\delta+}^{model}(R_p), \quad (3)$$

with  $A_{IA}(M)$  the amplitude of the intrinsic alignment signal,  $b_g(M)$  the cluster bias and  $w_{\delta+}^{model}(R_p)$  a function in which we include the dependence on  $R_p$  ([van Uitert & Joachimi 2017](#), equation 5); the dependence in the mass of the halo  $M$  is in both the  $A_{IA}(M)$  and  $b_g(M)$  factors.

We also use the LS ([Landy & Szalay 1993](#)) estimator to calculate the clustering signal:

$$\hat{\xi}_{gg}(R_p, \Pi) = \frac{D_d D_d - 2D_d R + RR}{RR}, \quad (4)$$

where  $D_d D_d$  represents the number of cluster pairs,  $D_d R$  the number of cluster - random point pairs, and  $RR$  the number of random point pairs. We then integrate along the line of sight to obtain the total projected clustering signal:

$$\hat{w}_{gg}(R_p) = \int_0^{\Pi_{max}} d\Pi \hat{\xi}_{gg}(R_p, \Pi). \quad (5)$$

We describe the clustering signal with a simple model:

$$w_{gg}(R_p, M) = b_g^2(M) w_{\delta\delta}^{model}(R_p), \quad (6)$$

with  $w_{\delta\delta}^{model}(R_p)$  a function in which we include the dependence on  $R_p$  ([van Uitert & Joachimi 2017](#), equation 9).

To get rid of the cluster bias  $b_g(M)$  factor and focus on the mass dependence of the amplitude  $A_{IA}(M)$ , we define:

$$r_{g+}(R_p, M) = \frac{w_{g+}(R_p)}{\sqrt{w_{gg}(R_p)}} = \frac{A_{IA}(M) w_{\delta+}^{model}(R_p)}{\sqrt{w_{\delta\delta}^{model}(R_p)}} \quad (7)$$

where we assume that the clustering signal  $w_{gg}(R_p)$  is positive, which is indeed true if we evaluate it at a reasonably small  $R_p = R_p^*$  - see Sect. for further discussion. If we evaluate the whole expression in Eq. 7 at this same value  $R_p^*$ , which we adopt to be the midpoint of a logarithmic bin which covers  $6 \text{ Mpc}/h < R_p < 30 \text{ Mpc}/h$ , we obtain the quantity:

$$r_{g+}(M) = r_{g+}(R_p = R_p^*, M) \propto A_{IA}(M) \quad (8)$$

where we stress that this quantity now only depends on the mass of the halo  $M$ . The goal of this paper is to study the dependence on the mass of the amplitude  $A_{IA}(M)$  by studying the quantity  $r_{g+}(M)$ : assuming that

$$A_{IA}(M) \propto M^\beta, \quad (9)$$

we can adopt the following model for  $r_{g+}(M)$ :

$$r_{g+}(M) = A \cdot M^\beta \quad (10)$$

with  $A$  a generic amplitude with no physical meaning, and  $\beta$  as in Eq. 9.

To achieve this goal, we select the objects of the catalogues described in Sect. 2 in  $n = 5$  logarithmic mass bins, between  $10^{11} M_\odot$  and  $10^{14} M_\odot$  for the MS and between  $10^{12.5} M_\odot$  and  $10^{15} M_\odot$  for the MXXL, we split them in  $N = 3^3 = 27$  sub-boxes based on their positions inside the cube of the respective simulation, and calculate  $w_{g+}$  and  $w_{gg}$  for each of the  $N$  sub-samples by replacing the integrals in Eq. 2 and 5 with a sum over 20 line-of-sight bins, each  $(\Pi_{max} - \Pi_{min})/20$  Mpc/h wide. The points showed in Fig. are the arithmetical mean of the  $N$  values for each mass bin, while the error bars are represented by the standard deviation of the values.

\*\*\*ARE WE SURE THAT THE DEFINITION OF THE VIRIAL MASS IS THE SAME IN BOTH THE SIMULATIONS? CAN'T FIND ANY REFERENCE FOR THE MILLENNIUM, BUT FOR THE MXXL THEY SAY CONVENTIONAL, SO IT SHOULD BE OK\*\*\*

We then perform a posterior analysis over the data to retrieve the values of  $A$  and  $\beta$ : according to Bayes' theorem, if  $\mathbf{d}$  is the vector of the data and  $\mathbf{p}$  the vector of the parameters,

$$P(\mathbf{p}|\mathbf{d}) \propto P(\mathbf{d}|\mathbf{p}) P(\mathbf{p}) \propto e^{-\frac{1}{2}\chi^2} P(\mathbf{p}) \quad (11)$$

with  $P(\mathbf{p}|\mathbf{d})$  the posterior probability,  $P(\mathbf{d}|\mathbf{p})$  the likelihood function,  $P(\mathbf{p})$  the prior probability and  $\chi^2 = (\mathbf{d} - \mathbf{m})^T \mathbf{C}^{-1} (\mathbf{d} - \mathbf{m})$ , with  $\mathbf{m}$  the vector of the model and  $\mathbf{C}^{-1}$  the precision matrix, the inverse of the covariance matrix  $\mathbf{C}$ . We assume flat, uninformative priors in the fit with ranges  $\log_{10} A \in [-1.7; -0.6]$  and  $\beta \in [0; 0.5]$ . We estimate the covariance matrix from the data as in [Taylor et al. \(2013\)](#):

$$\mathbf{C}_{\mu\nu} = \frac{1}{N-1} \sum_{i=1}^N (x_{i,\mu} - \bar{x}_\mu)(x_{i,\nu} - \bar{x}_\nu) \quad (12)$$

with  $\mu, \nu \in \{1, \dots, n\}$ ,  $\bar{x}_\mu = \frac{1}{N} \sum_{i=1}^N x_{i,\mu}$ , and  $x_{i,\mu} = r_{g+}(M)$  for each sub-box and each mass bin, as defined in Eq. 7. We then invert the covariance matrix and correct the bias on the inverse to obtain an unbiased estimate of the precision matrix, given by:

$$\mathbf{C}_{unbiased}^{-1} = \frac{N-n-2}{N-1} \mathbf{C}^{-1} \quad (13)$$

where we assume  $N > n+2$ . The results of the analysis are presented in Sect. 4.

The choice of  $n$  and  $N$  is constrained by many factors: first of all, if  $N$  is too large the single values of  $w_{gg}$  (and  $w_{g+}$ ) tend to fluctuate around the mean, thus increasing the error bar and sometimes plunging below 0, which is unacceptable for our choice of  $r_{g+}(R_p, M)$ , as specified after Eq. 7. Furthermore, we want  $n$  to be large enough to be capable of displaying the trend of the signals along the whole mass range chosen. Finally, we need to take  $n \ll N$  to avoid divergences related to the fact that we estimate the covariance from a finite number of samples ([Taylor et al. 2013](#)).

## 4 RESULTS AND DISCUSSION

We first show the trend of  $w_{g+}$  and  $w_{gg}$  with  $R_p$  for the lowest, middle and largest mass bin, for both the catalogues; note that around  $R_p = R_p^*$   $w_{gg}$  is always positive within the error bar, so that Eq. 7 always returns a real value.

## 5 CONCLUSIONS

The last numbered section should briefly summarise what has been done, and describe the final conclusions which the authors draw from their work.

## ACKNOWLEDGEMENTS

BJ acknowledges support by an STFC Ernest Rutherford Fellowship, grant reference ST/J004421/1.

## REFERENCES

Landy S. D., Szalay A. S., 1993, [ApJ](#), **412**, 64  
Taylor A., Joachimi B., Kitching T., 2013, [MNRAS](#), **432**, 1928  
van Uitert E., Joachimi B., 2017, preprint ([arXiv:1701.02307v1](#))

## APPENDIX A: SOME EXTRA MATERIAL

If you want to present additional material which would interrupt the flow of the main paper, it can be placed in an Appendix which appears after the list of references.

This paper has been typeset from a  $\text{\TeX/L\AA\TeX}$  file prepared by the author.